Mesoscale Circulations Forced by Melting Snow. Part II: Application to Meteorological Features

KIT K. SZETO

Department of Physics, University of Toronto, Toronto, Ontario, Canada

RONALD E. STEWART

Cloud Physics Research Division, Atmospheric Environment Service, Downsview, Ontario, Canada

CHARLES A. LIN

Department of Meteorology, McGill University, Montreal, Quebec, Canada

(Manuscript received 2 July 1987, in final form 13 November 1987)

ABSTRACT

Various authors have proposed that the cooling associated with melting precipitation contributes significantly to the dynamics of mesoscale precipitation systems. In this study, we use the numerical model described in Part I of this paper to investigate the effects of the cooling-by-melting mechanism in three specific situations: rain/snow boundaries, the production of deep 0°C isothermal layers, and the trailing stratiform region associated with mesoscale convective systems.

It is found that melting in the vicinity of a rain/snow boundary produces a thermally indirect mesoscale vertical circulation that may be responsible for enhanced precipitation near a rain/snow boundary. Melting in the presence of warm air advection above the melting layer and cold advection at and below it are necessary for producing deep 0°C layers within realistic times. The dynamic effects of cooling associated with melting and evaporation in the stratiform region of a mature squall line system produce a mesoscale circulation qualitatively similar to that recently reported in the literature.

1. Introduction

A growing realization has developed of the importance of melting on the dynamics of mesoscale systems. Melting affects the atmosphere in ways similar to that of sublimation or evaporation. All these processes extract latent heat from the environment. These diabatic cooling effects in turn induce perturbation pressure gradients which can modulate the local dynamics of the parent storm. Whereas the sublimation or evaporation of precipitation requires a subsaturated environment, melting of snowflakes commences whenever the particle surface temperature reaches 0°C. Therefore, the favorable environmental conditions for the occurrence of melting and sublimation/evaporation are different although they are subtly related (Matsuo and Sasyo 1981).

In Part I of this paper (Szeto et al. 1988, hereafter referred to as Part I), we studied numerically the general dynamic response of the atmosphere to melting snow. A "just saturated" environment has been assumed so that evaporation and condensation can be neglected. The numerical model used is two-dimensional, nonlinear and nonhydrostatic with an explicit Lagrangian formulation of the melting microphysics. It is found in Part I that melting associated with a banded precipitation system produced a thermally direct mesoscale circulation consisting of forced cold outflow beneath the melting level and a weaker return flow above. Superimposed on the nonlinear overturning were transient gravity waves and small-scale convective activities embedded inside the melting-induced 0°C isothermal layer. The resulting circulation had several characteristics of a sea breeze but of course was forced at midlevels rather than at the surface, as first noted by Lin and Stewart (1986). Significant velocity perturbations (horizontal perturbations of a few meters per second and vertical motions of a few tens of centimeters per second) were associated with these circulations. Since these circulations propagated away from the source region, the authors proposed that they might even modulate the storm dynamics at locations remote from the source region.

The dynamic effects of melting are expected to be of particular importance in several atmospheric situations. In this paper, we use the numerical model de-

Corresponding author address: Dr. Charles Lin, Dept. of Meteorology, McGill University, 805 Sherbrooke Street West, Montreal, Quebec H3A 2K6 Canada.

scribed in Part I to study three such situations. In section 2, the effects of melting on the mesoscale dynamics close to a rain/snow boundary are examined. Throughout this paper, a rain/snow boundary is defined to be the separation between rain and snow regions at the surface. In section 3, a mechanism for producing deep near 0°C isothermal layers with moderate precipitation rates is discussed. The mesoscale circulations driven by the cooling due to melting and evaporation in the stratiform rain region of a mesoscale convective system are investigated in section 4.

2. Rain/snow boundaries

In Part I, we studied the melting-induced circulations arising from precipitation fields in the absence of a basic horizontal temperature gradient. Model results show that no organized circulation is induced by the melting associated with stratiform precipitation extending over the whole horizontal domain. This is to be expected because the gradient of the horizontal perturbation pressure is zero in such cases.

If a basic synoptic-scale horizontal temperature gradient exists, organized melting-induced circulations can be realized in stratiform precipitation. This results from the horizontal variation of melting rate (and thus the cooling) in these situations. In particular, if the surface temperature becomes subfreezing in some region of the domain, a rain/snow boundary exists somewhere at the surface. Melting effects are expected to play an important role in the dynamics at the rain/snow boundary because the magnitude and the location (relative to the rain/snow boundary) of this forcing will persist throughout the duration of the precipitation.

By studying a few rain/snow boundary cases in southern Ontario, Stewart and King (1987) recently found that the deepest radar echoes and the coldest satellite-measured cloud top temperatures typically occur near the rain/snow boundary. Also, precipitation is organized into bands close to the boundary. Because essentially saturated conditions occurred in these cases so that evaporation was not significant, Stewart and King proposed that a melting-induced circulation was responsible for these observations of organized precipitation bands. Their inference has been tested with our numerical model and the results are discussed in this section.

Figure 1 shows the initial temperature and potential temperature fields for a typical simulation. There is a basic horizontal temperature gradient of 0.05°K km^{-1} in the x direction. Initial conditions satisfy both geostrophic and hydrostatic balance. The initial temperature field implies a strong basic upper level flow in the negative y-direction via the thermal wind relationship. A uniform precipitation rate of 2.0 mm h^{-1} is prescribed throughout the domain and there is no initial x-velocity. Stable conditions are prescribed throughout the domain. Since no evaporation and

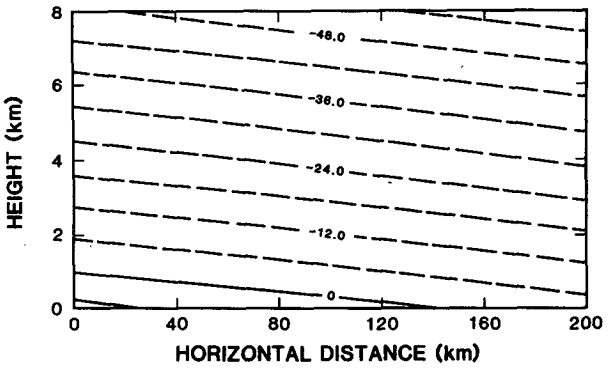

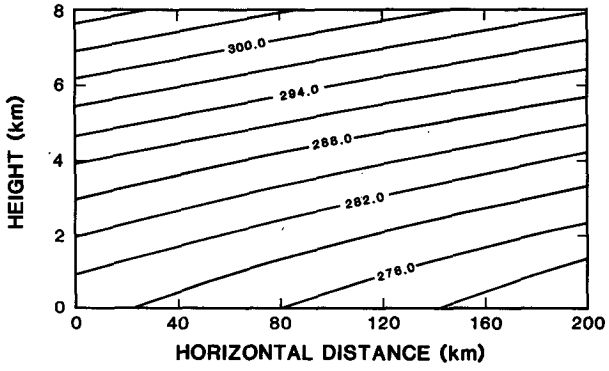

FIG. 1. (a) Initial temperature field (°C) for the rain/snow boundary run. (b) As in (a) except for potential temperature (°K). In this and other figures, the horizontal axis is in the x-direction.

condensation is considered, the melting level is located at the 0°C level.

Figure 2 shows the perturbation streamfunction field at t = 1 h and 3 h, respectively. The maximum perturbation x-velocities u' are confined to a small region just beneath the melting level. The maximum magnitude of u' achieved is about 2.5 m s^{-1}. There is a weak return flow above the 0°C level. Due to Coriolis effect, perturbation y-velocities v' ($\sim$1 m s^{-1} at t = 3 h) are generated in the negative y-direction in the melting layer. If the rain/snow boundary is long lasting, say 5 h or more, so that the Coriolis force has had enough time to act on the system, we would expect a low-level jetlike structure to develop in the negative y-direction in the rain region close to the boundary (with $v' \sim$ a few meters per second; see the linear steady-state results of Lin and Stewart 1986).

Substantial vertical motion is induced by the circulation. At 1 h, the updraft is located essentially in the "rain" region (surface temperature above 0°C) and is close to the rain/snow boundary. At 3 h, the updraft extends into the snow region beyond x = 140 km. The maximum updraft velocity developed is about 2 cm

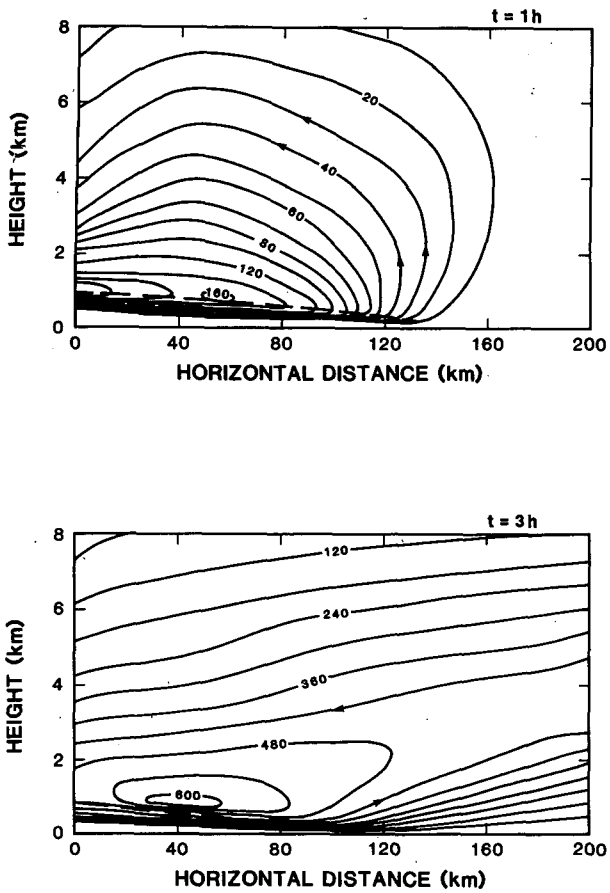

FIG. 2. Perturbation streamfunctions for the rain/snow boundary run (a) at $t = 1$ h. (b) At $t = 3$ h. The unit is kg $(m^2\ s)^{-1}$ and the 0°C isotherm is indicated by the heavy dashed line.

s^{-1} for the conditions used. At 3 h, forced downdrafts of the order of 10 cm s^{-1} are produced beneath the 0°C level in the rain region. The melting-induced circulation here is thermally indirect; descent is occurring on the "warm" side of the rain/snow boundary and ascent is occurring on the "cold" side of the boundary.

Due to the diabatic cooling of melting at low levels, the rain/snow boundary edge moves towards the negative x-direction into the original rain region. It is located at $x \sim 100$ km at $t = 3$ h and has therefore moved at a speed of approximately 4 m s^{-1} towards the rain region, a value consistent with the predictions of Stewart and McFarquhar (1987). Due to adiabatic warming along the descending branch below the 0°C level and warm advection by the perturbation horizontal velocities, the movement of the rain/snow boundary is somewhat slower than one would expect by considering the cooling by melting alone.

If the atmosphere is less stable (see Fig. 1 for the stratification in the present case) or if condensational heating is included, then the updraft speeds could easily exceed 10 cm s^{-1}. For example, if neutral lapse rates are prescribed in the lower levels, model results show that the maximum updraft magnitude reaches 20 cm s^{-1} within 1 h. Such updraft motions are of comparable magnitude to the values observed in cyclonic storm banded features (for example, see Browning and Harrold 1969). The horizontal extent of the circulation in neutral conditions is also less than in stable conditions with the same forcing. These model results provide strong support for the speculations of Stewart and King (1987) that organized circulations having vertical motions sufficient to affect precipitation fields are expected in the region of the rain/snow boundary.

Model results predict that surface parameters will systematically change across the rain/snow boundary. Winds will back in passing from the boundary into the snow region due to the reduction of the magnitudes of v' in the snow region. In the transition from rain to snow, there will also be an accentuated temperature fall. Moreover, there is a positive (hydrostatic) pressure perturbation beneath the melting level in the rain region away from the rain/snow boundary and a negative (nonhydrostatic) pressure perturbation in the vicinity of the boundary (note the location of low-level outflow and the location of surface convergence near $x = 105$ km in Fig. 2). The above considerations show that the melting driven circulations at the rain/snow boundary should have a frontal-like character.

Observations made during the Canadian Atlantic Storms Program (CASP) field project (Stewart et al. 1987) support these model predictions. As shown in

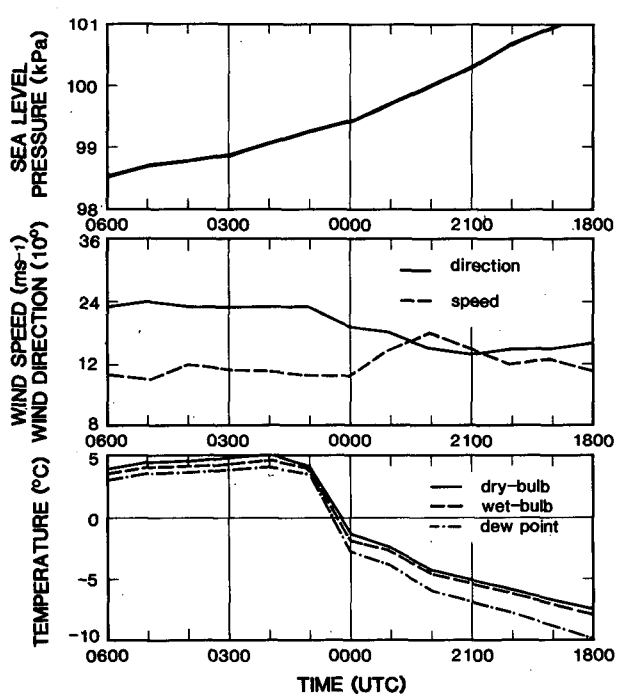

FIG. 3. Surface parameters at St. John's, Newfoundland on 11–12 March 1986. Rain was occurring at temperatures above 0°C and freezing rain, ice pellets and snow were occurring at subfreezing temperatures.

the typical results of Fig. 3, a rapid temperature change occurred as temperatures passed through 0°C. The rate of change of surface pressure also increased when passing from the rain to the snow region (note that if the synoptic-scale surface pressure gradient is positive in the vicinity of the rain/snow boundary, like the case here, the melting-induced perturbation pressure field discussed above will imply an increase in horizontal gradient of total pressure in crossing the boundary). These transitions were associated with a backing wind from the rain to snow region. Nearly saturated conditions, implying very little evaporation, occur during such transitions.

In Fig. 2b, we see that the updraft (and associated adiabatic cooling) occurs on the "cold" side of the boundary and the downdraft (and associated adiabatic warming) occurs on the "warm" side of the boundary. Moreover, an examination of Fig. 1 and Fig. 2 shows a convergence of the horizontal heat flux $u'T$, where T is the basic temperature, on the warm side of the rain/snow boundary. These model results suggest that the melting-induced circulation at a rain/snow boundary is frontogenic in the low levels. Using a simple model of a rain/snow boundary that only considered the energy absorbed from the air due to melting, Stewart and McFarquhar (1987) suggested that the rain/snow boundary can either be frontogenic or frontolytic. Further observational and modeling efforts are needed before more definitive statements can be made about this aspect of the rain/snow boundary.

When we compare Figs. 2a and b with Fig. 1b, we see that as a function of time, the streamlines (except in the melting layer) become more aligned with the isentropic surfaces, especially away from the rain/snow boundary, which results in the updraft extending into the snow region.

In attempting to explain this tilting behavior, we note that the solution to the set of Eqs. (1)–(5) of Part I includes the symmetric instability modes (Bennetts and Hoskins 1979). Symmetric instability occurs when air parcel motion advects y-momentum and potential temperature at different rates, thereby producing geostrophic imbalance. The most unstable parcel displacement for symmetric instability is the one that is close to the isentropic surface. Thus, if symmetric instability occurs in the solution, it will be superimposed on the melting-induced circulations to yield the observed behavior.

In the absence of horizontal shear, the condition for symmetric instability is that

$$\mathrm{Ri} \equiv N^2/(\partial v/\partial z)^2 < 1 \qquad (1)$$

where Ri is the Richardson number, N is the Brunt–Väisälä frequency and z is the height. In the idealized basic state of the present simulation, Ri is less than unity almost everywhere due to the strong vertical shear associated with the basic y-velocities. Thus, symmetric instability is very likely to occur in the present simulation.

As pointed out by Bennetts and Hoskins (1979), without the effect of condensation, symmetric instability rarely occurs in the real atmosphere because Ri is usually much larger than unity. However, model results show strong vertical shear induced by melting in the lower levels. Hence, with the Richardson number criterion, it is inferred that the dynamic effects of melting may produce conditions favorable for the occurrence of symmetric instability. Because of their potential importance in organizing midlatitude mesoscale precipitation systems, further investigations of the coupling between melting-induced dynamics and symmetric instability are warranted.

3. Deep 0°C isothermal layers

Both observations and numerical results show that the depth of 0°C isothermal layers resulting from the melting associated with light to moderate precipitation is typically limited to a few hundred meters (Stewart et al. 1984 and Part I). However, deep 0°C isothermal layers having depths up to 1 km or more have also been observed (Stewart 1984). Due to the enhanced static stability in these deep isothermal layers, they must significantly affect the storm dynamics near their locations.

Since the temperature of these deep isothermal layers is close to or at 0°C, it is believed that melting contributes substantially to their development. Assuming an initial lapse rate of 6°C km^{-1} and a rainfall rate of 1 mm h^{-1}, Stewart (1984) showed that a 1 km-deep isothermal layer at 0°C would be formed in $\approx$10 h under optimal static conditions. This information indicates that the diabatic effect of melting often cannot alone account for the formation of these isothermal layers because precipitation has not lasted long enough.

Figure 4 shows an illustrative sounding recently made during the CASP field project. The deep near 0°C layer extended over a depth of about 23 kPa. Essentially saturated conditions existed at levels below 65 kPa. Hence, sublimation/evaporation effects did not contribute to the maintenance of this layer. Unfortunately, the sounding before the onset of precipitation was not available. Therefore, the contribution of evaporative cooling to the formation of this layer is not clear.

Observations (Stewart 1984 and Fig. 4) show that strong wind shear occurs throughout these deep 0°C isothermal layers. In the cases cited, the wind field had a strong northerly or northeasterly component in the low levels and a strong southerly or southeasterly component at the top of these layers. With temperature decreasing towards the north in all cases, the wind shear indicates warm advection at the upper portion of the 0°C layer and cold advection beneath it.

Numerical results show that deep 0°C isothermal

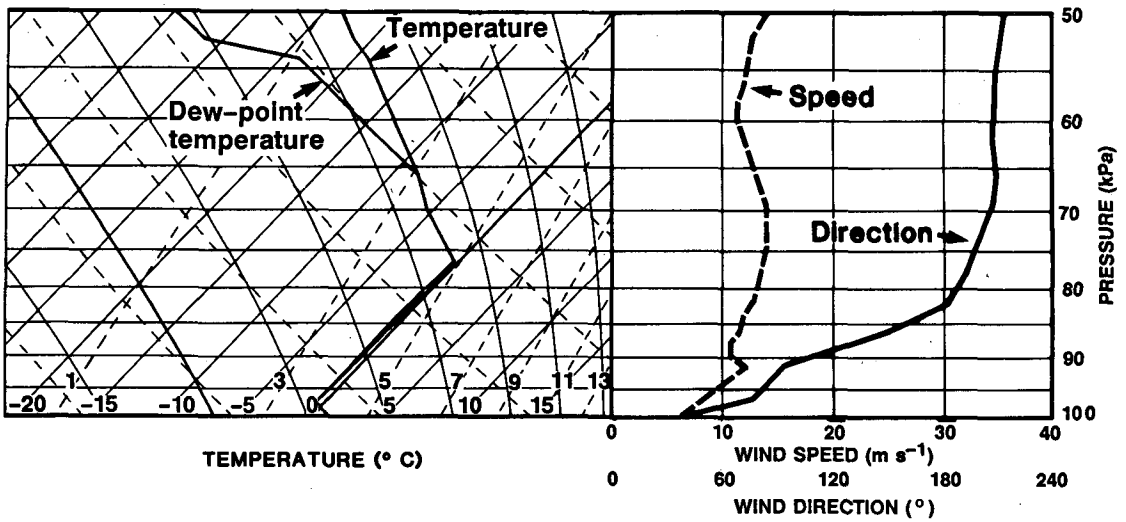

FIG. 4. Temperature sounding and wind profile observed at 1327 UTC 22 February 1986 from Shearwater, Nova Scotia during the CASP field project.

layers can be formed in a reasonably short time from the melting of light snowfall in such an environment. Using the vertical wind profile shown in Fig. 5, Fig. 6a shows the evolution of such a deep isothermal layer in a typical simulation. In this simulation, a precipitation rate of 2 mm h^{-1} has been prescribed throughout the model domain. There is a horizontal temperature gradient of $-0.05°C\ km^{-1}$ in the x-direction. Horizontal temperature gradients of this magnitude are common in frontal zones. A near 0°C isothermal layer close to 1.5 km deep was formed in 100 min from melting in this light precipitation rate.

Without the differential temperature advection, the depth of the resultant isothermal layer is about 300 m (see Part I). There are two reasons for producing deep near 0°C isothermal layers. First, warm air advection at levels above the initial melting level raises the temperature to above 0°C so melting will commence in these layers. Only a small amount of snow needs to melt in this formerly subfreezing region in order to force the temperature back down to 0°C. That is, a deep 0°C isothermal layer is one result of the competing effects of warm air advection and melting at regions above the initial melting level. Second, low-level cold air advection beneath the melting layer will decrease the air temperature in this region. Consequently, less snow needs to be melted in order to cool these lower layers to 0°C than would be the case without advection.

Without the diabatic effects of melting, the differential temperature advection discussed above leads to the formation of inversions having maximum temperatures above 0°C (Fig. 6b). Such temperature profiles are essential for freezing precipitation formation. Even with melting, it is quite conceivable that strong warm air advection will result in an inversion having temperatures greater than 0°C. It is suggested therefore that the production of deep 0°C isothermal layers should commonly be associated with freezing precipitation formation. Observational evidence from the indicated CASP case as well as from other CASP observations supports this suggestion. Within 15 min of the 22 February 1986 sounding (Fig. 4), ice pellets were observed at the surface. These particles only occur through the partial melting of snow aloft (Stewart 1985), implying that an inversion having temperatures above 0°C must have developed shortly after the sounding with the 23 kPa deep 0°C layer was made.

In Part I (as well as in the results presented in section 2), we observed that the melting-induced horizontal flow reversed its direction near the 0°C level. These perturbation winds therefore produce altered temperature advections near the rain/snow boundary. De-

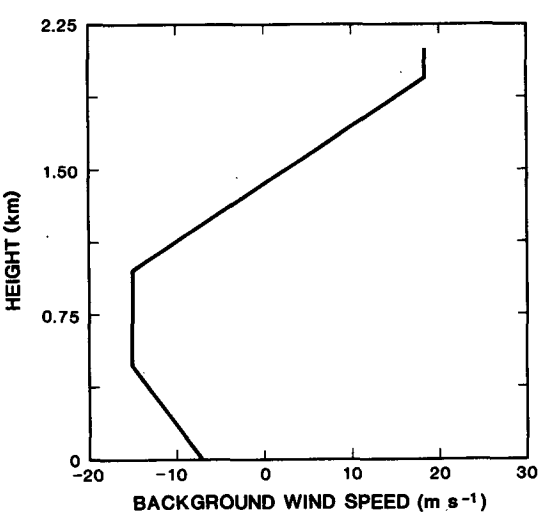

FIG. 5. The vertical profile of the horizontal (x) wind for the numerical simulation of a deep 0°C layer.

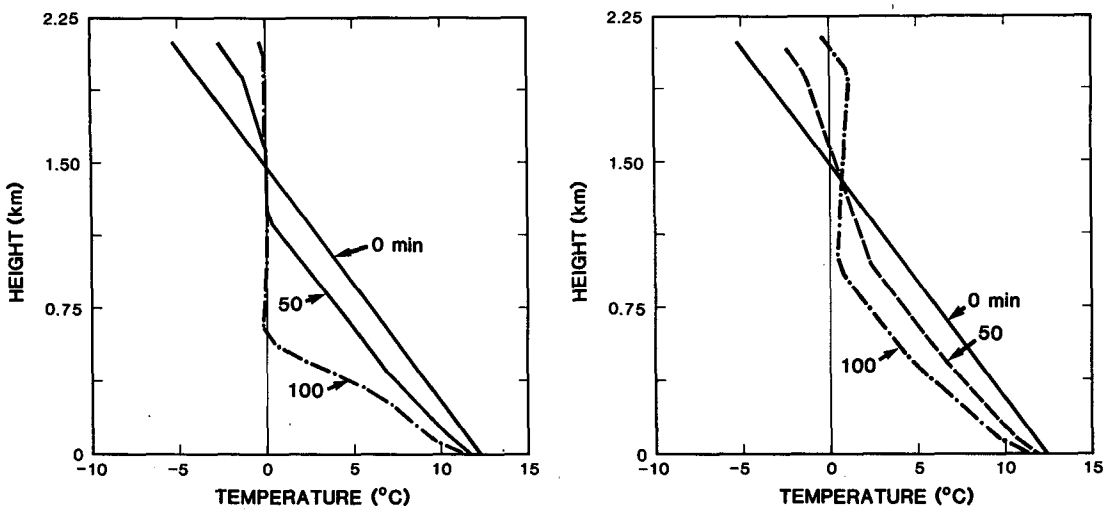

FIG. 6. Temporal evolution of the temperature profile in the presence of (a) both melting and temperature advection and (b) without melting. The 0°C isotherm is indicated with a light solid line.

pending on the three-dimensional background temperature field, this local temperature advection may itself contribute to the production of deep 0°C isothermal layers or upper level inversions. It is thus suggested that in the vicinity of the rain/snow boundary, the melting-induced circulation can alter the dynamics and thermodynamics significantly enough to affect precipitation types (rain, snow, freezing precipitation, and/or ice pellets).

4. Mesoscale circulations in convective systems

Observational studies reveal that mesoscale convective systems show substantial mesoscale organization (for example, see Leary and Houze 1979; Smull and Houze 1985, 1987; Srivastava et al. 1986; Chong et al. 1987; Knupp and Cotton 1987). Common characteristics have been found in some of these studies. In a mature squall line system, stratiform cloud and light precipitation typically cover an extensive region behind the leading convective elements. It has been found that there is often an ascending front-to-rear (FTR) flow relative to the storm motion in this stratiform region. Below this system of FTR flow there is a layer of rear-to-front (RTF) flow which descends through the melting layer and progressively penetrates into the region of the convective towers. These two opposite currents may collide and result in mesoscale convergence and vertical motions in the stratiform region. Convergence is frequently observed immediately above the 0°C level with divergence beneath it. A salient feature of these circulations is that upper-level mesoscale updrafts and underlying mesoscale downdrafts usually take place with the separation height between these drafts located near the melting level.

The origin of these mesoscale circulations and their influence on the life cycle of the convective systems are currently the focus of substantial research. Since the 0°C level is often found to be a characteristic level delineating flow regimes in these circulations, it is suggested that the cooling associated with melting and evaporation plays an important role in the dynamics of these mesosystems. Some of the dynamic effects of melting and evaporation in these stratiform regions have been investigated by using our present model.

Since condensation has not been incorporated in our model, no attempt is made to simulate the full evolution of a convective system. Instead, we consider only

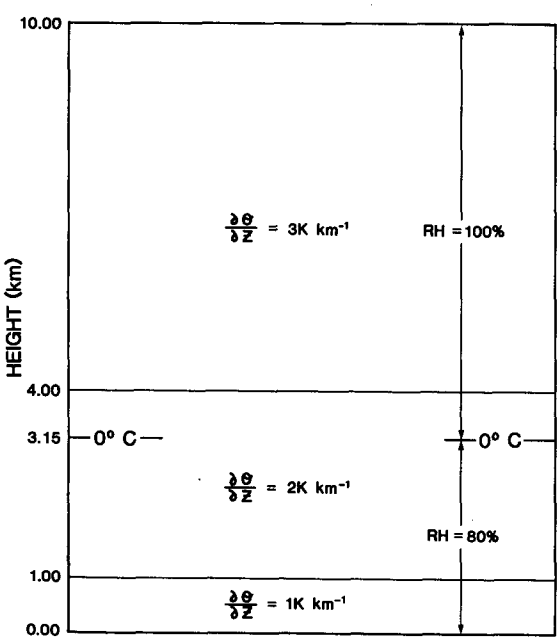

FIG. 7. Initial stratification for the model runs presented in Figs. 8 and 9.

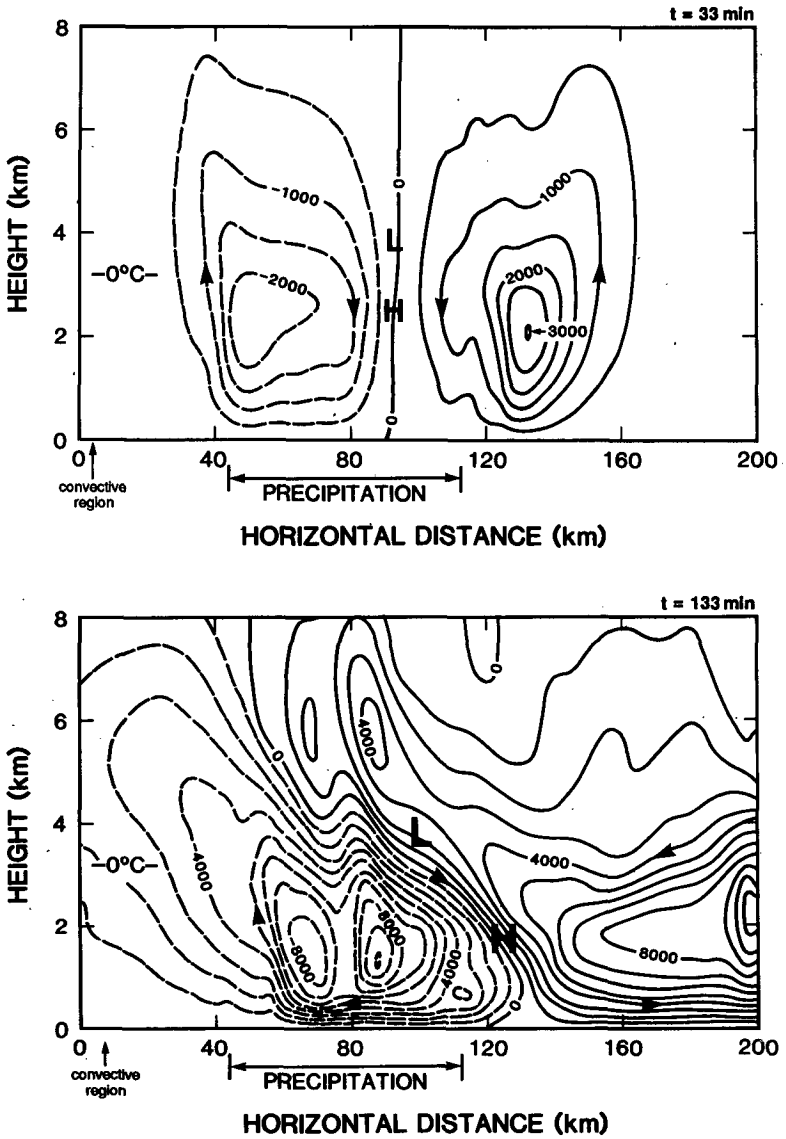

FIG. 8. Perturbation streamlines for the stratiform region of a convective system with both melting and evaporation included. The times illustrated are (a) 33 min and (b) 133 min. The contour intervals are (a) 500 kg $(m^2\ s)^{-1}$ and (b) 1000 kg $(m^2\ s)^{-1}$. The initial 0°C level and the horizontal extent of the precipitation field are also indicated. The low and high perturbation pressure centers are indicated by L and H.

the trailing stratiform region of these convective systems. Moreover, this stratiform region is assumed to be already formed at the initial time and is isolated from the convective region so that the dynamic coupling between the two is neglected. The treatment of sublimation and evaporation of precipitation particles is similar to that outlined in Beard and Pruppacher (1971). Moisture conservation with evaporation as the source term has also been incorporated in this set of experiments.

The precipitation rate is 5 mm h^{-1} throughout the region 44 km $< x <$ 112 km and zero elsewhere in the simulation presented here. Initial relative humidity is 80% beneath the 0°C level and 100% above this level. A mean wind of 10 m s^{-1} in the positive x-direction is introduced to simulate a storm-relative basic flow. The atmosphere is initially stable throughout the domain (Fig. 7) and there is no initial horizontal temperature gradient. The convective region is assumed to be located to the left (in the negative x-direction) of the stratiform precipitation.

At the early stage of the simulation, the induced circulations are concentrated near the edges of the precipitation region (Fig. 8a). There is generally descending motion below the 0°C level within the precipitation. At later times (Fig. 8b), the circulation becomes much

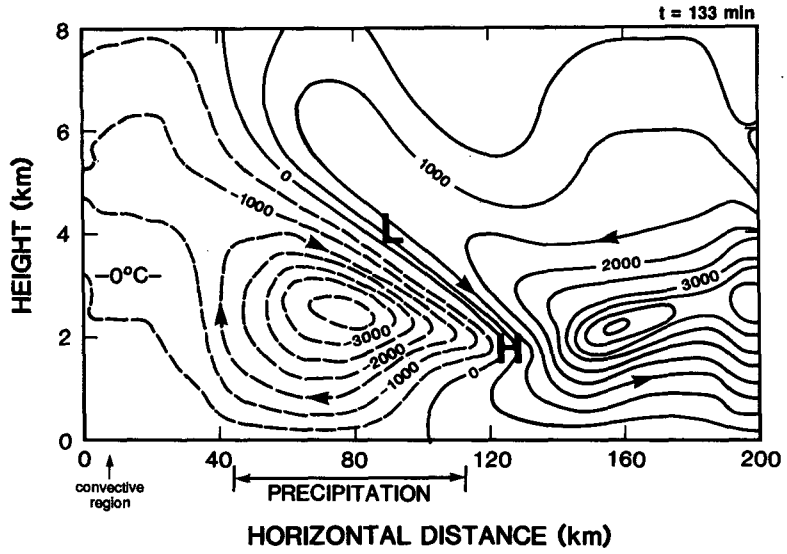

FIG. 9. As in Fig. 8b except without evaporation. Contour interval is 500 kg $(m^2 s)^{-1}$.

more intense. In agreement with observations, there is strong convergence above the 0°C level near the trailing end of the precipitation pattern. A FTR current is induced above the 0°C level in the front to midregion of the precipitation pattern. A strong RTF component traverses the melting layer and attains maximum strength at the low levels in the front region of the stratiform precipitation. This RTF jet is fed by the air converging into the low pressure center located immediately above the 0°C level near the rear of the precipitation region. Positive pressure perturbations beneath the 0°C level result in divergence in this region. The downdraft speed reaches 1.5 m s^{-1} and the maximum horizontal perturbation velocity reaches 20 m s^{-1} at t = 133 min. Detailed discussions of the basic dynamics associated with such a circulation have been presented in Part I and will not be repeated here.

Figure 9 shows the result for a similar run but with only the effects of melting included. The overall circulation is very similar to that previously discussed. The RTF jet is more confined to the melting layer and the circulations are less intense.

Table 1 summarizes the sensitivity of the model results to the effects of melting and/or evaporation. For the atmospheric conditions considered, the results suggest that the effects of melting are comparable to those of evaporation in driving these mesoscale circulations. With both melting and evaporation included, the effects are stronger than those which result from the mere additive effects of the individual ones. This indicates the nonlinear nature of the response of the atmosphere to these diabatic forcings.

TABLE 1. Comparison of the effects of different forcing. Initial conditions used in these runs were identical to those used for the run of Fig. 8 except without the background flow and using a stratiform precipitation rate of 3 mm h^{-1}. The u', w' and ψ' are perturbation horizontal velocity, perturbation vertical velocity and perturbation streamfunction, respectively.

	Melting + evaporation	Melting only	Evaporation only
max$\lvert w'\rvert$ (m s^{-1})	0.72	0.18	0.33
max$\lvert u'\rvert$ (m s^{-1})	10.00	2.80	6.00
max$\lvert\psi'\rvert$kg $(m^2 s)^{-1}$	7560	2200	4700

There are certainly qualitative similarities between the model results and observed circulations (see the reports cited above). Of course, exact quantitative comparisons between model results and observations are impossible because of, for example, the neglected effects of three-dimensionality and condensation in our model. Vertical velocities may be overestimated in our model results due to the two-dimensionality of the model. The inclusion of condensational heating is believed to be essential in the numerical simulation of the mesoscale updrafts above the melting level. If surface friction and the cold outflow that flows into the stratiform region from the convective region have been included in the model, we would have expected the RTF jet to be more elevated from the surface, as suggested by observations. Nevertheless, the model results do strongly suggest that the cooling associated with melting contributes significantly to the characteristics of these mesoscale circulations.

5. Summary and conclusions

In the preceding sections, the dynamic consequences of melting have been examined numerically for three specific situations. The results of these simulations are as follows.

It was found that the melting of snow induces a thermally indirect mesoscale circulation in the vicinity of a rain/snow boundary. Such a circulation has an updraft branch near the rain/snow boundary. These results support the idea of Stewart and King (1987) that the heavy precipitation near a rain/snow boundary is a consequence of melting-induced circulations.

It was shown that melting in a strong shear environment produces the deep (>1 km) 0°C isothermal layers that are observed. The isothermal layers result from the differential temperature advection in the vicinity of the melting layer and the cooling-by-melting mechanism. Preliminary observations and model results also support the contention that an imbalance between the temperature advection and melting terms can lead to freezing precipitation.

The dynamic effects of melting and evaporation in the trailing stratiform regions of mature squall lines have been examined. Model results show that the cooling associated with melting and evaporation of precipitation falling from the extensive stratiform region is an important contributing mechanism for dynamic processes on the mesoscale. Melting is essential for realistic simulation of these mesoscale fields.

The preceding three illustrations point out that the ice-phase microphysics must be incorporated in the numerical studies of at least these mesoscale weather systems. Our model is clearly limited by its two-dimensionality and its inability to describe completely the interaction between the mesoscale and the convective and/or larger scales. However, we believe that it is important to isolate the cooling-by-melting forcing in order to understand its dynamic effects on various weather systems. In this respect, our results demonstrate the critical role of melting in the explanation of phenomena observed in both winter and summer storms.

Acknowledgments. This work was supported by the Atmospheric Environment Service (AES), the Federal Panel on Energy Research and Development (PERD), the Natural Sciences and Engineering Research Council (NSERC) and the University of Toronto.

REFERENCES

Beard, K. V., and H. R. Pruppacher, 1971: A wind tunnel investigation of the evaporation of small water drops falling at terminal velocity in air. *J. Atmos. Sci.*, **28,** 1455–1464.

Bennetts, D. A., and B. J. Hoskins, 1979: Conditional symmetric instability—a possible explanation for frontal rainbands. *Quart. J. Roy. Meteor. Soc.*, **105,** 945–962.

Browning, K., and T. W. Harrold, 1969: Air motion and precipitation growth at a cold front. *Quart. J. Roy. Meteor. Soc.*, **96,** 369–389.

Chong, M., P. Amayenc, G. Scialom and J. Testud, 1987: A tropical squall line observed during the COPT 81 experiment in West Africa. Part I: Kinematic structure inferred from dual Doppler radar data. *Mon. Wea. Rev.*, **115,** 670–694.

Knupp, K. R., and W. R. Cotton, 1987: Internal structure of a small mesoscale convective system. *Mon. Wea. Rev.*, **115,** 629–645.

Leary, C. A., and R. A. Houze, Jr., 1979: Melting and evaporation of hydrometeors in precipitation from the anvil clouds of deep tropical convection. *J. Atmos. Sci.*, **36,** 661–679.

Lin, C. A., and R. E. Stewart, 1986: Mesoscale circulations initiated by melting snow. *J. Geophys. Res.*, **91,** 13299–13302.

Matsuo, T., and Y. Sasyo, 1981: Melting of snowflakes below freezing level in the atmosphere. *J. Meteor. Soc. Japan,* **59**(1), 10–24.

Smull, B. F., and R. A. Houze, Jr., 1985: A midlatitude squall line with a trailing region of stratiform rain: Radar and satellite observations. *Mon. Wea. Rev.*, **113,** 117–133.

——, and ——, 1987: Dual Doppler radar analysis of a midlatitude squall line with a trailing region of stratiform rain. *J. Atmos. Sci.*, **44,** 2128–2148.

Srivastava, R. C., T. J. Matejka and T. J. Lorello, 1986: Doppler radar study of the trailing anvil region associated with a squall line. *J. Atmos. Sci.*, **43,** 356–377.

Stewart, R. E., 1984: Deep 0°C isothermal layers within precipitation bands over southern Ontario. *J. Geophys. Res.*, **89,** 2567–2572.

——, 1985: Precipitation types in winter storms. *Pure Appl. Geophys.*, **123,** 597–609.

——, and P. King, 1987: Rain/snow boundaries over southern Ontario. *Mon. Wea. Rev.*, **115,** 1894–1907.

——, and G. M. McFarquhar, 1987: On the width and motion of a rain/snow boundary. *Water Resour. Res.*, **23,** 343–350.

——, J. D. Marwitz, J. C. Pace and R. E. Carbone, 1984: Characteristics through the melting layer of stratiform clouds. *J. Atmos. Sci.*, **41,** 3227–3237.

——, R. W. Shaw and G. A. Isaac, 1987: Canadian Atlantic Storms Program: The meteorological field project. *Bull. Amer. Meteor. Soc.*, **68,** 338–345.

Szeto, K. K., C. A. Lin and R. E. Stewart, 1988: Mesoscale circulations forced by melting snow. Part I: Basic simulations and dynamics. *J. Atmos. Sci.*, **45,** 1629–1641.